# Vortex structure around a magnetic dot in planar superconductors

I. K. Marmorkos, A. Matulis,* and F. M. Peeters
*Department of Physics, University of Antwerp (UIA), B-2610 Antwerpen, Belgium*
(Received 31 May 1995; revised manuscript received 20 September 1995)

The problem of the giant vortex state around a magnetic dot which is embedded in a superconducting film is investigated. The full nonlinear, self-consistent Ginzburg-Landau equations are solved numerically in order to calculate the free energy, the order parameter of the host superconductor, the internal magnetic field due to the supercurrents, the corresponding current density, the magnetization probed in the vicinity of the dot, and the normal electron density as a function of the various parameters of the system. We find that, as we increase the magnetic moment of the dot, higher flux quanta vortex states become energetically more favorable, as they can better compete with the external magnetic field via the Meissner effect. In addition to that, they progressively become closer to each other in energy with direct experimental consequences, i.e., physical quantities like magnetization may fluctuate when measured, for example, as a function of a uniform external magnetic field.

## I. INTRODUCTION

It is well known that a crucial factor determining the usefulness of a superconductor in practical applications is the maximum current at which it can operate (critical current). This current is very small for type-I superconductors. In type-II superconducting materials, however, large critical currents have been measured which makes them more favorable for applications in, e.g., superconducting magnets. In those materials the magnetic field lines partially penetrate the superconductor and transform it into the Abrikosov state by forming a hexagonal lattice of vortices.[1,2] The magnetic field lines penetrate the core of each vortex where the material is in the normal state, whereas, the rest of the system remains superconducting. The application of a bias voltage results in motion of these vortices giving rise to dissipation which is now the limiting factor for the largeness of the critical current of the superconductor.[3,4]

To get around the above problem, and substantially enhance the critical current, it is required to pin the Abrikosov lattice as strongly as possible. Defects in the crystal of size in the order of the superconducting coherence length $\xi$ are very effective in vortex pinning.[5] Experimentally, several types of defects have been utilized so far in studying vortex pinning: e.g., point defects[6] and amorphous columnar defects[7,8] created after bombarding the superconducting material with high energy ions.

Since a full control over pinning is desirable, artificially fabricated submicrometer holes in superconducting films have been recently studied experimentally.[9] For certain ''matching'' fields, where the period of the Abrikosov vortex lattice and that of the lattice of holes were multiple of each other, a strong pinning of vortices was found which resulted in a strong enhancement of the critical current and in sharp peaks in the magnetization curves.[9] An alternative route exploited by van Roy *et al.*[10] was to grow a lattice of magnetic dots made of $\tau$-MnAl on top of the superconducting film. At temperatures close to the transition temperature $T_c$ a strong increase in the magnetization was measured, when the dots were magnetized, indicating an enhanced pinning of the fluxoids by the modulated magnetic field of the dots.

In the present work, we focus on the later system and study in detail via the Ginzburg-Landau (GL) formalism how the superconducting film is perturbed in the neighborhood of the magnetic dots. The paper is organized as follows: In the following Sec. II we describe the model on which our study is based. Section III discusses the technicalities of the numerical integration of the nonlinear Ginzburg-Landau equations. In Sec. IV, we present and discuss our results. Our results are summarized in Sec. V.

## II. MODEL

To better understand the behavior of this system, experimentally studied by van Roy *et al.*,[10] we start from the simplest possible theoretical model that, we believe, captures the qualitative aspects of the physics involved. We consider a single magnetic dot of radius $R$ embedded in a planar superconductor occupying the infinite $x$-$y$ plane and characterized by a Ginzburg-Landau parameter $\kappa=\lambda/\xi$, and thermodynamic critical field $H_c$. $\lambda$ is the penetration depth of the superconducting material in question and $\xi$ is its coherence length. The only source of external field applied to the superconductor is provided by the magnetic dot whose magnetic moment $\vec{m}$ is directed along the positive $z$ axis and which gives rise to a vector potential which, on the $x$-$y$ plane, takes the form

$$\vec{A}_0(\vec{r})=(H_c\lambda)\frac{\chi}{2\kappa}A_0(r)\vec{e}_\theta, \tag{1}$$

where we introduced the dimensionless vector potential

$$A_0(r)=\left(\frac{2m}{\chi^3}\right)\frac{4}{k}\frac{1}{\sqrt{r}}\left[\left(1-\frac{k^2}{2}\right)K(k)-E(k)\right]. \tag{2}$$

Here and further we shall use the unit vectors of the polar coordinate system: $\vec{e}_x$, $\vec{e}_\theta$, and $\vec{e}_z$. In the above expression, as well as in the rest of this work, we express distance in units of the radius of the dot $R=\chi\xi$ ($\chi$ is the dimensionless radius of the dot in units of the superconducting coherence length $\xi$), the magnetic field in units of $H_c$, and the

 

magnitude of the magnetic moment $m$ of the dot in units of $m_0=H_c(\pi\xi^3)$. $K(k)$ and $E(k)$ are complete elliptic integrals of the first and second kind, respectively, with $k=4r/(1+r)^2$. We should notice that on the plane of the superconductor the corresponding magnetic field $\vec{H}_0(r)=\vec{\nabla}\times\vec{A}_0(r)$ points along the negative $z$ axis, for this particular choice of the magnetic moment $\vec{m}=m\vec{e}_z$ of the dot. In order to limit the number of parameters we assumed an infinite thin magnetic dot when we calculated the vector potential (2).

We consider the magnetic dot, on top of the superconducting plane, to be made of a hard magnet of uniform magnetization and that the structure of its internal diamagnetic currents, which gives rise to its macroscopic magnetic moment $m$, is not affected by the possible presence of nearby circulating supercurrents. That is, we realize a magnetic dot with rigid magnetic properties which serves only as a source for the external nonuniform field $A_0(r)$ on the superconducting plane. The magnetic lines of this field penetrate the plane of the superconductor normally, have a radial symmetry, and decrease in strength as we move away from the dot giving rise to a magnetic dipole field $[H_0(r)\sim m/r^3]$ at large distances. Near the vicinity of the dot, however, the radial dependence of this nonuniform field on the $x$-$y$ plane is more complicated, and is given by a combination of elliptic integrals [see Eq. (2)], whereas at the edge of the disk is logarithmically divergent, since both the superconductor and the magnetic dot are realized on the same $x$-$y$ plane. An alternative way to create the same magnetic field is by using a circular loop with the same radius $R$ carrying a current $I=mc/(\pi R^2)$. The advantage of the later system is that this externally imposed magnetic field can be tuned in a controlled way by changing the current on the loop. The fabrication of such current loops should be feasible nowadays with the advances in nanolithographic techniques.

The physical properties of the superconductor under consideration are well described by the Ginzburg-Landau theory[1,2] which reduces to the equations

$$\frac{1}{2m}\left(-i\hbar\vec{\nabla}-\frac{2e\vec{A}}{c}\right)^2\psi+\alpha\psi+\beta|\psi|^2\psi=0 \tag{3}$$

and

$$\vec{j}=\frac{e\hbar}{im}(\psi^*\vec{\nabla}\psi-\psi\vec{\nabla}\psi^*)-\frac{4e^2}{mc}\psi^*\psi\vec{A}. \tag{4}$$

The first equation gives the order parameter $\psi$ and the second one the supercurrent (diamagnetic response) of the superconductor. In the absence of any external fields, the order parameter takes the constant value $\psi=\psi_0$ which is determined by the density $n_s$ of Cooper pairs in the system. The second equation, which is nothing more than the usual quantum-mechanical expression for the current in an external field, should be coupled to the Maxwell equation $\vec{\nabla}\mathrm{x}\vec{H}=(4\pi/c)\vec{j}$. For a complete and consistent description of the properties of the superconducting plane under the external field $\vec{A}_0(\vec{r})$ the two nonlinear Ginzburg-Landau equations, coupled together with the above Maxwell equation, should be solved self-consistently with the appropriate boundary conditions. For a superconductor-insulator interface, the theory of Ginzburg and Landau requires the supercurrent across the interface to vanish, that is

$$\left(-i\hbar\vec{\nabla}-\frac{2e}{c}\vec{A}(r)\right)_n\psi=0. \tag{5}$$

For the sake of convenience we write the total internal vector potential $\vec{A}(r)$ in the superconductor as

$$\vec{A}(r)=(H_c\lambda)\left(\frac{\chi}{2\kappa}\right)\left[A_0(r)+\frac{1}{r}\phi(r)\right]\vec{e}_\theta, \tag{6}$$

where the dimensionless function $\phi(r)$ is obtained from the self-consistent solution of the Ginzburg-Landau equations, and is directly related to the vector potential created by the internal currents in the superconductor.[11] The corresponding total magnetic field $\vec{H}(r)=\vec{\nabla}\times\vec{A}(r)$ is given by

$$\vec{H}(r)=H_c\left(H_0(r)+\frac{1}{2r}\frac{d\phi}{dr}\right)\vec{e}_z, \tag{7}$$

where the second term on the right-hand side of the above equation is the magnetic field created by the supercurrents.

The radially symmetric magnetic field $H_0(r)$ created by the magnetic dot gives rise to superconducting vortices with size determined by the size of the dot. These vortices correspond to circulating currents around the dot and form the so-called ''giant vortex state'' (Refs. 11,12) which is closely related to the superconducting surface state. It differs from the mixed state since it can carry a total current, whereas the ideal Abrikosov state (without pinning centers) cannot.[13,14] Because of the circular symmetry of our problem we take the order parameter of the form $\psi(r,\theta)=F(r)\exp(iL\theta)$. The single valueness of $\psi$ forces the constant $L$ to be an integer. The correspondence of $L$ to the orbital angular momentum quantum number, considering $\psi(r,\theta)$ to be a wave function in the Schrödinger-like Eq. (3), is evident, and, in our system, it can be associated with the number of fluxoids penetrating the superconducting annulus region defined by the edge of the magnetic dot and the circulating giant vortex.

A circulating current loop, with radius $r$ and current density $\vec{j}(r)$, gives at $r+x$ rise to a magnetic field $\vec{h}(r+x)$ such that $|\partial h_z/\partial r|/|\partial h_r/\partial z|\sim 1/x$, with $x\to 0$. Therefore, for our particular problem of the giant vortex state, which results from a circulating current density, we can safely reduce Maxwell's equation $\vec{\nabla}\times\vec{h}(r)=(4\pi/c)\vec{j}(r)$ to $-\partial h_z/\partial r=(4\pi/c)j(r)$, and write the two Ginzburg-Landau equations in the final dimensionless form

$$\frac{1}{r}\frac{d}{dr}\left(r\frac{dF(r)}{dr}\right)=\left(\frac{\chi^2}{2\sqrt{2}\kappa}\right)^2\left[A_0(r)+\frac{1}{r}[\phi(r)-B]\right]^2F(r)-\chi^2F(r)[1-F^2(r)] \tag{8}$$

and

$$\frac{d}{dr}\left(\frac{1}{r}\frac{d\phi(r)}{dr}\right)=\left(\frac{\chi}{\kappa}\right)^2\left[A_0(r)+\frac{1}{r}[\phi(r)-B]\right]F^2(r), \quad (9)$$

with $B=(2\sqrt{2}\kappa/\chi^2)L$. In our model the magnetic dot serves *only* as the source of the external, nonuniform field acting on the superconductor which is bounded by the magnetic disk. Thus we assume hard wall boundary conditions between the magnetic dot and the superconductor, and no magnetic field lines due to supercurrents are allowed to penetrate it. If we notice that the magnetic field of a current loop is much stronger close to the circumference of the loop, and drops fast, as we move towards the center of the loop, we expect that this is not such a bad approximation, which greatly facilitates our calculation.

Under these assumptions, the boundary condition expressed by Eq. (5) is translated into $dF(r)/dr=0$ at $r=R$. From Eq. (6), however, it follows that the vector potential $A_s(r)$ due to supercurrents is $A_s(r)\sim\Phi(r)/r$ and, in accordance with our assumptions for the properties of the hard wall at the edge of the dot, the usual definition of the magnetic flux $\Phi_s=\oint\vec{A}_s d\vec{l}$ at $r=R$ gives $\phi(R)=0$. At large distances from the edge of the dot the normalized order parameter $F(r)$ assumes the full value of the complete Meissner superconducting state, that is $F(r)=1$, whereas, from the asymptotic expansion of Eqs. (8) and (9) we find, for $r\gg R$, $\phi(r)-B\sim(2\pi m/\chi^3)/r^2$. The corresponding field $H_s(r)$ created by the supercurrents becomes $H_s(r)\sim(2\pi m/\chi^3)/(2r^3)$, and exactly cancels the field $H_0(r)$ of the magnetic dot. Matching the numerical solutions of the above equations to these asymptotic expressions at $r\gg R$ we naturally recover the complete Meissner state of the plane superconductor at large distances from the dot.

According to the above consideration we arrived at the following boundary conditions:

$$dF(r)/dr=0|_{r=R}, \quad \phi(R)=0 \quad (10)$$

and

$$F(r)\to 1 \text{ and } \phi(r)-B\to(2\pi m/\chi^3)/r^2, \text{ when } r\to\infty. \quad (11)$$

## III. NUMERICAL INTEGRATION

We integrated numerically the system of two ordinary differential equations (8), (9) with the boundary conditions (10) and (11). This is a nonlinear two point boundary value problem. We discovered that the integration cannot be done straightforwardly, and consequently, some kind of iteration technique should be used.

We constructed a superconvergent method which is based on the relaxation technique (see, for example, Ref. 15). The details of this method are given in the Appendix, while the main result of it is the replacement of the nonlinear set of equations (8) and (9) by the following linear set of equations for the successive approximates:

$$\frac{d}{dr}F_{n+1}=\frac{1}{r}G_{n+1},$$

$$\frac{d}{dr}G_{n+1}=\alpha_{00}F_{n+1}+\alpha_{01}\Phi_{n+1}+\beta_0,$$

$$\frac{d}{dr}\Phi_{n+1}=r\Psi_{n+1},$$

$$\frac{d}{dr}\Psi_{n+1}=\alpha_{10}F_{n+1}+\alpha_{11}\Phi_{n+1}+\beta_1 \quad (12)$$

with

$$\alpha_{00}=r\alpha\left(A_0(r)+\frac{\Phi_n(r)}{r}\right)^2-r\chi^2[1-3F_n^2(r)],$$

$$\alpha_{01}=2\alpha\left(A_0(r)+\frac{\Phi_n(r)}{r}\right)F_n(r),$$

$$\alpha_{10}=2\beta\left(A_0(r)+\frac{\Phi_n(r)}{r}\right)F_n(r),$$

$$\alpha_{11}=\frac{\beta}{r}F_n^2(r),$$

$$\beta_0=-2\alpha\left(A_0(r)+\frac{\Phi_n(r)}{r}\right)F_n(r)\Phi_n(r)-2r\chi^2F_n^3(r),$$

$$\beta_1=-\beta\left(A_0(r)+2\frac{\Phi_n(r)}{r}\right)F_n^2(r), \quad (13)$$

where $\Phi_n=\phi_n-B$, $\alpha=[\chi^2/(2\sqrt{2}\kappa)]$, and $\beta=(\chi/\kappa)^2$. The boundary conditions (10) and (11) are linear and they remain the same for the above iterative scheme.

The obtained two point linear boundary problem is much more simple. We integrated it straightforwardly using the standard supplementary function technique (see, for example, Ref. 16). Namely, we integrated the above nonhomogeneous linear equation set and the analogous homogeneous equation set twice with the boundary conditions, and then matched the result with the asymptotic function behavior (11). We took particular care at the starting point ($r=R$) were the vector potential $A_0(r)$ logarithmically diverges. To properly handle this divergence, we used the asymptotic expansion of Eqs. (12) to analytically advance their solution in the first step of the integration. We found out that the method was really superconvergent, and that typically five to six iterations were sufficient.

## IV. RESULTS AND DISCUSSION

A crucial physical quantity that determines the behavior of the vortex state around the magnetic dot, as a function of the various parameters of the system, is the difference of the total magnetic free energy between the superconducting and the normal state which is given by

$$\int \Omega_{SH}dV-\int \Omega_{NH}dV=\frac{H_c^2}{8\pi}\int[(H(r)-H_0(r))^2-F^4(r)]dV. \quad (14)$$

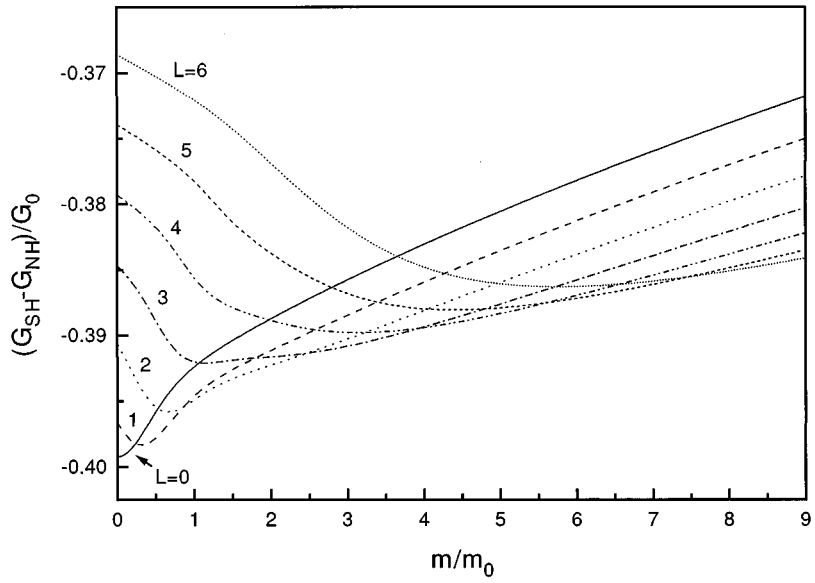


FIG. 1. Free energy difference between the normal and superconducting state ($\kappa=1$) of our system as a function of the magnetic moment $m$ of the dot for various flux quanta numbers $L$. $G_0=10^3(H_c^2/8\pi)(\pi\xi^2)$, $m_0=H_c(\pi\xi^3)$, and the magnetic dot has a radius $R=\xi$.

In our case, we are interested in the contribution of the giant vortex state to the free energy, which we refer to the free energy of the uniform superconducting plane (where the magnitude of that difference acquires the constant value of $H_c^2/8\pi$ per unit volume). Therefore, we calculated the above integral over an annulus region of space defined between $r=R$ and $r_c=20R$. All the physics we are interested in (giant vortex state) takes place within this region for all sets of parameters we investigated. Our conclusions are not sensitive to the particular choice of $r_c$ as long as $F(r_c)\simeq 1$ (i.e., we include all the region spanned by the corresponding vortex state, whereas the calculation of the above integral from $r_c$ to infinity merely would add an unimportant constant).

Relevant results for the free energy difference as a function of the magnetic moment $m$ of the dot are shown in Fig. 1 for different quantum numbers $L$. Here, we consider a superconducting material with a Ginzburg-Landau parameter $\kappa=1$ and a magnetic dot with radius $R=\xi$. The vortex state with the quantum number $L$ which gives the lower free energy difference is the one that is physically realized. In our system of a nonuniform external magnetic field, we have checked that such a state of a minimum total free energy gives rise to a free energy density which is lowest everywhere in space. This is shown explicitly in Fig. 2 for the $m=1$ case. From Fig. 1 we see that for a particular value of $m=m_{c_1}$ the complete Meissner state ($L=0$) ceases to be energetically the most favored one, and a vortex state containing one flux quantum appears. This value of $m_{c_1}$ corresponds to the lower critical field $H_{c_1}$ we have in the case of the *uniform* external field. A further increase of $m$ eventually introduces one more fluxoid in the system, and so on. From our results we see that in the low $m$ regime the various vortex states associated with different flux quanta $L$ are energetically well distinct from each other. At larger $m$ values, however, states with different $L$ are very close together in

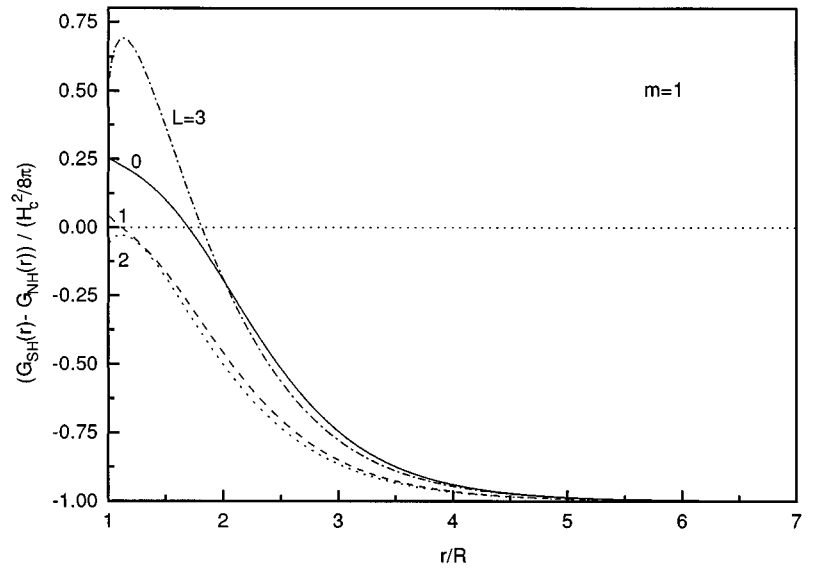


FIG. 2. Free energy density difference between the normal and superconducting state ($\kappa=1$) of our system as a function of distance from the edge of the dot, which has a magnetic moment $m=1$, and radius $R=\xi$, for various flux quanta numbers $L$.

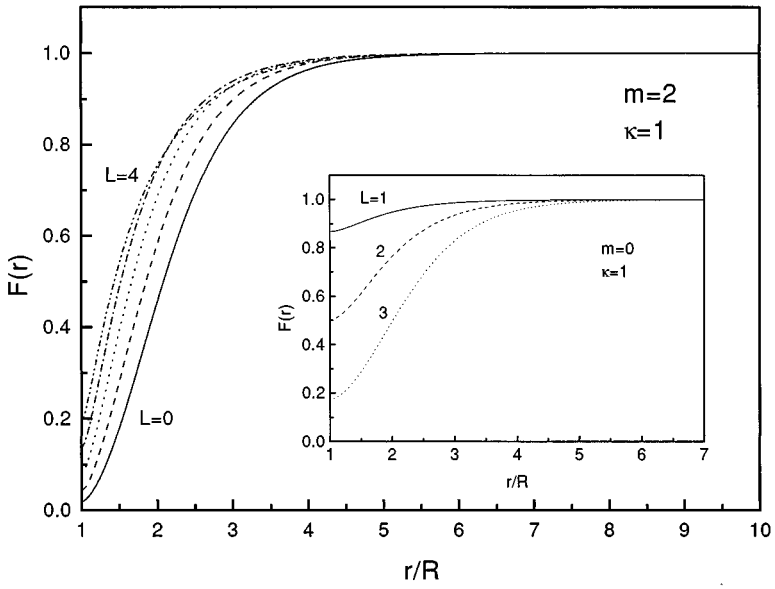


FIG. 3. Order parameter $F(r)$ of our superconducting system with $\kappa=1$ as a function of the distance from the edge of the dot, which has a magnetic moment $m=2$ (inset $m=0$), and radius $R=\xi$, for various flux quanta numbers $L$.

energy, and, consequently, the system can easily make transitions from one vortex state to another one with a different quantum number $L$. This may result in fluctuations when measuring various physical quantities of the system (magnetization) as a function of some external parameter, i.e., an additional uniform, external magnetic field. In fact, such peculiar fluctuations have been observed experimentally,[10] and the mechanism we described could serve as a guide of thought in trying to better understand them. This means that at large magnetic moments of the dot, where the resulting field is higher, the order parameter of the system is not a simple function of one $L$ component only, but it should be written as a superposition

$$\psi=\sum_L F_L(r)e^{iL\theta}. \tag{15}$$

The larger the magnetic moment of the dot, the more $L$ components are expected to have an important contribution in the above summation. In this case, the system has a finite probability to be in any one of those states characterized by a particular quantum number $L$. At low values of the magnetic moment of the dot, however, our simple model of keeping only one $L$ component is more accurate, whereas, at larger $m$ values it still captures all the qualitative aspects of the physics involved.

In Fig. 3 we present results for the order parameter $F(r)$ in the superconducting plane as a function of distance from the edge of the magnetic dot. Our results refer to a superconductor with $\kappa=1$, and to a dot that has a magnetic moment $m=2$ and radius $R=\xi$. The inset shows similar results but for $m=0$. For the above set of parameters, we plot $F(r)$ for different values of the flux quantum number $L$. First of all, we see from the inset of Fig. 3 that for $m=0$, vortex states with lower $L$ values assume a higher value of the order parameter. We have checked that the state with $L=0$ has the highest order parameter, $F(r)=1$, everywhere in space. From Fig. 1 we notice that this state gives a lower free energy and energetically is the most favored at $m=0$. Close to the edge of the dot the values of $F(r)$ for different $L$ are well distinct from each other, and, within a distance of about $5R$, $F(r)$ approaches unity, as is the case for the uniform Meissner state. The transition of $F(r)$ to unity is rather broad, and, the larger $L$ is, the larger the required distance for $F(r)$ to reach unity. At higher magnetic fields, (see Fig. 3) the state with $L=0$ has now a drastically lower order parameter which is a consequence of the fact that the $L=0$ vortex state is no longer energetically favored (see Fig. 1). In the case of higher fields, we notice that the order parameters for different $L$ values are closer to each other, especially the ones for larger $L$. The reduction of the superconducting state [lower $F(r)$] close to the edge of the magnetic dot is more pronounced now, whereas, the transition of $F(r)$ to unity is noticeably sharper compared to the $m=0$ case.

Figure 4 depicts similar results for the order parameter $F(r)$, but for a superconductor that has a larger Ginzburg-Landau parameter $\kappa=3$ and a magnetic dot with $m=2$. We get qualitative similar behavior with the one we had for the lower value of $\kappa=1$ at lower magnetic fields, however. For example, we have checked that the results for the order parameter with $m=2$ and $\kappa=3$ show similar qualitative trends to the ones with $m=1$ at $\kappa=1$. That is, increasing $\kappa$, the behavior of the superconducting system scales at higher magnetic field values. Thus our model recovers the well known fact that superconductors with a higher Ginzburg-Landau parameter $\kappa$ exhibit, at higher magnetic fields, the same behavior which others (with lower $\kappa$ values) show at lower fields, i.e., assume higher critical magnetic fields.[1,2]

In Fig. 5 we plot results for the current density of the supercurrents as a function of the distance from the magnetic dot with $m=5$ ($m=1$ in the inset) over different values of the flux quantum number $L$ characterizing the corresponding giant vortex state. First of all, notice that the circulating internal currents change direction at a particular distance $r$, from being negative to positive. Thus there are two currents circulating in opposite direction. This phenomenon is similar to the behavior of bulk cylindrical superconductors under a uniform external magnetic field.[11] From our results of Fig. 5

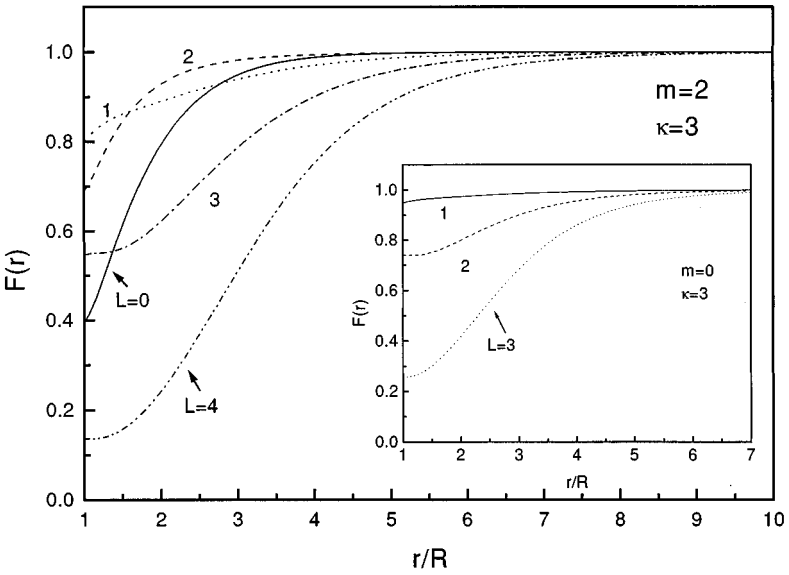


FIG. 4. Order parameter $F(r)$ for the same system as in Fig. 3 but now for $\kappa=3$.

we see that, for higher $m$, states with lower flux quanta give rise to current densities that have a negative sign of circulation over larger distances, resulting finally in a total current of negative sign. According to the choice of our unit vectors, a negative sign in the internal current indicates that the corresponding magnetic field created by the superconductor points in the same direction as the external field $H_0(r)$ of the magnetic dot. Such currents cannot compete and screen effectively the external field, and are totally unable to give rise to the Meissner effect. From Figs. 1 and 5 we notice that, for a particular value of $m$, flux states with extensive regions of negative internal currents are energetically less favored. For example, we see from the inset of Fig. 5 that for $m=1$ and $L=2$ the corresponding current density is positive over an extensive region of space and gives rise to a total current which is able to generate the Meissner effect. At the same time (see Fig. 1) this state is energetically more favored to the one with $L=1$ which lacks these features. For $m=5$ states with larger $L$ give rise to circulating currents that better screen the external field and more effectively minimize the free energy of the superconducting system. The $L=4$ state is the one with the lowest free energy for $m=5$. If we conventionally identify the positive peak of the current density as indicating an effective radius $r_v$ of the system of the magnetic dot along with the circulating giant vortex, we find that $r_v$ decreases as the system makes a transition to higher $L$ states. According to our results in Fig. 1 these transitions take place more easily at higher $m$ values and finally results in fluctuations of the effective radius $r_v$. For $m=5$, $r_v$ could fluctuate between the states with $L=4$ and 5 resulting in fluctuations over distances up to $R/2$, with direct experimental consequences. For example, the application of an additional uniform external magnetic field would result in fluctuations of the magnetization as a function of the magnitude of this field.[10]

The circulating internal currents around the magnetic dot,

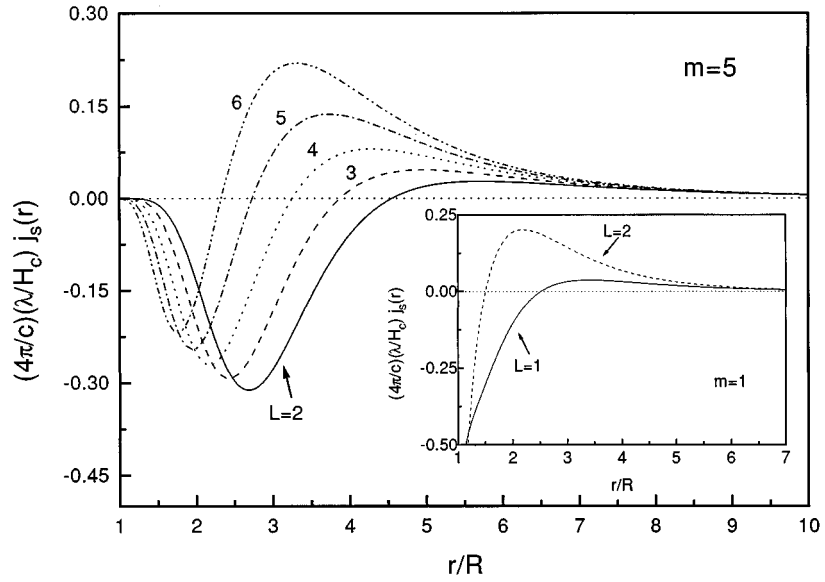


FIG. 5. Current density profile in the superconductor as a function of the distance from the edge of the dot which has a magnetic moment $m=5$ (inset $m=1$) and radius $R=\xi$ for various flux quanta numbers $L$. The corresponding superconductor has a GL parameter $\kappa=1$.

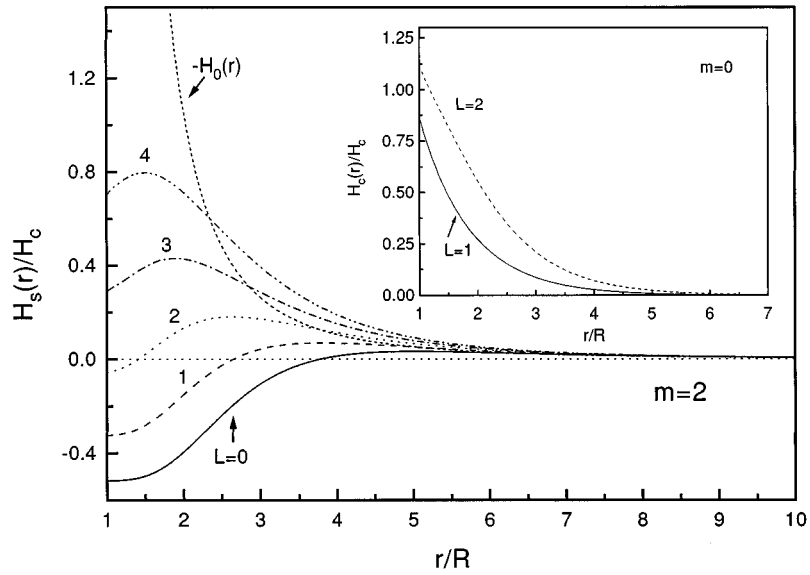


FIG. 6. Magnetic field profile generated by the supercurrents as a function of distance from the edge of the dot, which has a magnetic moment $m=2$ (inset $m=0$), and radius $R=\xi$, for various flux quanta numbers $L$. The corresponding superconductor has a GL parameter $\kappa=1$. The external magnetic field $H_0(r)$ due to the magnetic dot is also shown.

which form the giant vortex state, give rise to a magnetic field $H_s(r)$ whose direction depends on that of the associated supercurrent. The region in space over which the circulating current inverts direction could also be a pronounced feature of the corresponding magnetic field profile. To further investigate this, we show in Fig. 6 the magnetic field $H_s(r)$ created by these circulating currents as a function of the distance from the edge of the dot for $m=2$ for different flux quantum numbers $L$. The inset shows similar results but for $m=0$. First of all, we notice from the inset for $m=0$ that $H_s(r)$ decreases monotonously from the edge of the dot, being lower for lower $L$ values, and approaching zero at distances where the corresponding order parameters approach unity. The picture for the higher $m=2$ field value, however, looks different in Fig. 6. The magnetic field $H_s(r)$ for low values of $L$ is negative for distances close to the edge of the magnetic dot, becomes positive at intermediate, and reduces to zero at larger distances from the dot. A negative sign of the field $H_s(r)$ indicates that its direction is the same as the one of the applied external field. However, only when $H_s(r)$ is positive in sign can it compete with the external field and give a reduced total internal magnetic field (Meissner effect). From Fig. 6, however, and for $m=2$ we see that vortex states with a higher flux quantum number $L$ give rise to a field which is positive over a much larger distance, and, along with their more effective competition with the external magnetic field, they give rise to a lower free energy of the system. We have, finally, checked that the peak in $H_s(r)$ is exactly associated with the point where the corresponding supercurrent inverts direction. In Fig. 6 we plot also the external magnetic field $H_0(r)$ created by the magnetic dot in order to demonstrate how this field is exactly canceled at large distances by $H_s(r)$ in order to recover the complete Meissner state of the uniform planar superconductor. From the energy diagram of Fig. 1 we see that the vortex state with $L=2$ is the one with the lowest free energy at

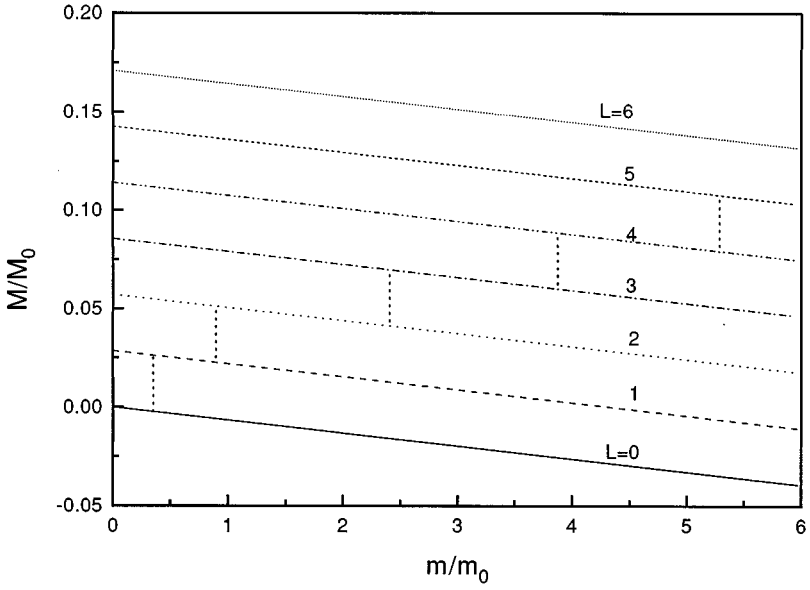


FIG. 7. Total magnetization in a region defined between the edge of the dot and $r_0=10R$ as a function of the dimensionless magnetic moment $m$ of the dot, which has a radius $R=\xi$, for various flux quanta numbers $L$. $4\pi M_0=10^2 H_c(\pi\xi^2)$. The vertical lines indicate the transition points between the different $L$ states as dictated by the minimum of the free energy.

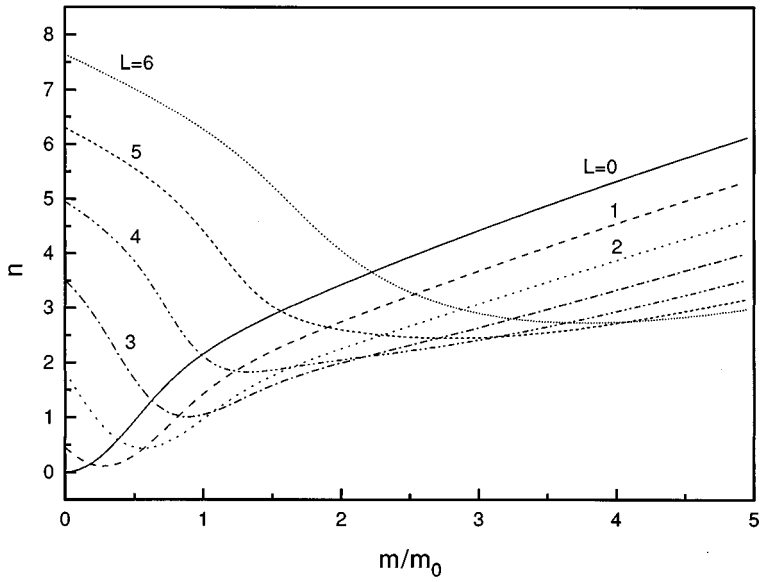


FIG. 8. Number of normal electrons $n$ as a function of the dimensionless magnetic moment $m$ of the dot, which has a radius $R=\xi$, for various flux quanta numbers $L$.

$m=2$, and, according with our results in Fig. 6, this state better cancels the external field $H_0(r)$ over a larger distance.

The internal circulating currents in the superconducting region around the magnetic dot give rise to a magnetization $4\pi M(r)=H_c(H(r)-H_0(r))$. The average value of it, in a finite region of space around the dot, can be directly probed experimentally using a superconducting quantum interference device. A common outcome of such experimental measurements is a hysteretic behavior of the magnetization, as a function of the externally applied magnetic field,[17] indicating that the superconducting system prefers to conserve the total number of flux quanta trapped in it over a finite range of the external magnetic field. Sometimes this may happen even at the cost of overriding the condition of minimum free energy over a finite range of the external field.[11] In Fig. 7 we show results for the total magnetization of a superconducting region spanned in a distance up to $10R$, as a function of the magnetic moment $m$ of the dot over different flux quanta numbers $L$. We notice the linear behavior of the magnetization as a function of $m$. Transitions between lines of different $L$ take place at certain values of $m$. If the condition for minimum energy dictates the behavior of the magnetization, such transitions take place at the values of $m$ indicated by the vertical dotted lines in Fig. 7. Under the condition of minimum energy requirement, the magnetization changes reversibly. The same holds over a finite interval of $m$ such that the system moves along a line of fixed $L$. If the system, however, prefers to conserve the number of flux quanta at larger ranges of $m$, even at the cost of overriding the condition for minimum energy imposed by Fig. 1, then a hysteretic behavior of the magnetization appears. In that case, an increase of $m$ over an appropriate, finite interval, followed by a decrease back to zero leaves a certain number of flux quanta locked around the magnetic dot.

In Fig. 8 we plot $n=\int_R^\infty(1-F^2)rdr$, which is proportional to the total number of normal electrons in the $x$-$y$ plane, as a function of the magnetic moment $m$ over different quantum numbers $L$. We see that, as we increase the externally applied non-uniform magnetic field (i.e., increase $m$), the superconducting region around the dot progressively decreases. This shows up in Fig. 8 as an increase of the number of normal electrons $n$ as we increase $m$. After a careful comparison with the energy diagram of Fig. 1, we note that this increase in $n$ always occurs for $L$ states that are physically realizable (i.e., have a lower free energy) at the particular value of $m$ we are considering. We also notice that, at small values of $m$, $L$ states that have the minimum normal electron density are well separated from each other. At larger $m$, however, states with higher $L$, which according to the results in Fig. 1 are energetically more favored, have normal electron densities closer to each other.

## V. SUMMARY AND CONCLUSIONS

As a summary, we studied the giant vortex state around a magnetic dot embedded in a superconducting film. We found that at low values of the magnetic moment $m$ of the dot vortex states with a low number $L$ of flux quanta associated with them are energetically more favored and well separated from each other in energy. At large $m$ values, however, vortex states with a larger $L$ are now more favored, whereas, they are quite close together in energy. We pointed out that this may result in fluctuating physical quantities when, for example, we drive the system with some uniform external magnetic field. In fact, such peculiar fluctuations may be related to the ones which have been observed in magnetization measurements for a lattice of magnetic dots on top of a superconducting film.[10]

## ACKNOWLEDGMENTS

Stimulating discussions with V. V. Moshchalkov and W. Van Roy are acknowledged. This work was supported by the Belgian National Science Foundation, by NATO through the linkage Grant No. 950274, and by the PHANTOMS network (ESPRIT Basic Research Action 7360).

## APPENDIX: SUPERCONVERGENT RELAXATION TECHNIQUE

The nonlinear two point boundary problem is a complicated numerical problem and cannot be handled straightfor-

wardly. Here we present some general consideration which allows to reduce it to a linear iterative scheme. We shall illustrate our consideration by applying it to a first order nonlinear differential equation set which we formally present as

$$\frac{d}{dx}f=H(f). \tag{A1}$$

Here, the symbol $f$ stands for some vector function with components $f=\{f_1(x),\ldots,f_n(x)\}$, and $H(f)$ is some nonlinear function of that vector. We shall also assume that proper boundary conditions accompany Eq. (A1). The two point boundary conditions are given at the different points $x_i$.

The above equation set (A1) is rather general, as every system of ordinary differential equations can be reduced to an equivalent set of first order differential equations. Moreover, other equations (e.g., integral equation) can often be presented in the form analogous to Eq. (A1).

The main idea of the relaxation technique is the following. Instead of solving Eq. (A1) defined on the $x$ axis we shall consider another equation

$$\frac{\partial}{\partial t}\left\{\frac{\partial}{\partial x}f-H(f)\right\}=-\left\{\frac{\partial}{\partial x}f-H(f)\right\}, \tag{A2}$$

which is defined in the $xt$ plane. When $t\to\infty$ its solution converges to the solution of our basic Eq. (A1). For the sake of simplicity we shall assume that the boundary conditions of our basic problem are linear and append them to Eq. (A2). We like to point out, however, that in the case of nonlinear boundary conditions they can be handled in the same way, just replacing them by the relaxation equations analogous to Eq. (A2).

Now we shall replace the time derivative in Eq. (A2) by the approximate expression

$$\frac{\partial}{\partial t}f\approx\frac{f(t+h)-f(t)}{h}\approx\frac{f(t+1)-f(t)}{1}=f_{n+1}-f_n \tag{A3}$$

and

$$\frac{\partial}{\partial t}H(f)=\frac{\partial H}{\partial f}\frac{\partial}{\partial t}f\approx\frac{\partial H}{\partial f}(f_{n+1}-f_n), \tag{A4}$$

where $(\partial H/\partial f)f$ stands for

$$\frac{\partial H}{\partial f}f=\sum_{i=1}^{n}\frac{\partial H}{\partial f_i}f_i(x). \tag{A5}$$

Finally, substituting expressions (A3) and (A4) into Eq. (A2) and restricting ourselves to linear terms in $(f_{n+1}-f_n)$ only, we obtain the following set of equations:

$$\frac{d}{dx}f_{n+1}-H_f(f_n)f_{n+1}=H(f_n)-H_f(f_n)f_n, \tag{A6}$$

which is the required linear iteration scheme for our basic problem (A1).

Now denoting the derivatives of $F(r)$ and $\Phi(r)$ by $G(r)/r$ and $\Psi(r)r$, respectively, and applying the above considerations to Eqs. (8) and (9), we immediately arrive at the iteration scheme given by Eqs. (12).

*Permanent address: Semiconductor Physics Institute, Gostauto 11, 2600 Vilnius, Lithuania.

[1] A. A. Abrikosov, *Fundamentals of the Theory of Metals* (North-Holland, Amsterdam, 1988).

[2] P. G. de Gennes, *Superconductivity of Metals and Alloys* (Addison-Wesley, New York, 1989).

[3] M. Tinkham, Phys. Rev. Lett. **13**, 804 (1964).

[4] Y. B. Kim, C. F. Hempstead, and A. R. Strnad, Phys. Rev. **131**, 2486 (1963); **139**, A1163 (1965).

[5] R. P. Huebener, *Magnetic Flux Structures in Superconductors* (Springer-Verlag, Berlin, 1979), and references therein.

[6] A. I. Larkin and Y. N. Ovchinnikov, J. Low Temp. Phys. **34**, 409 (1979).

[7] L. Civale, A. D. Marwick, T. K. Worthington, M. A. Kirk, J. R. Thompson, L. Krusin-Elbaum, Y. Sum, J. R. Clem, and F. Holtzberg, Phys. Rev. Lett. **67**, 648 (1991); W. Gerhauser *et al.*, *ibid.* **68**, 879 (1992).

[8] A. I. Bazdin, Phys. Rev. B **47**, 11 416 (1993); G. S. Mkrtchyan and V. V. Shmidt, Sov. Phys. JETP **34**, 195 (1972).

[9] V. V. Moshchalkov, L. Gielen, M. Baert, V. Metlushko, G. Neuttiens, C. Strunk, V. Bruyndoncx, X. Qiu, M. Dhalle, K. Temst, C. Potter, R. Jonckheere, L. Stockman, M. V. Bael, C. V. Haesendonck, and Y. Bruynseraede, Phys. Scr. **T55**, 168 (1994); V. V. Metlushko, M. Baert, R. Jonckheere, V. V. Moshchalkov, and Y. Bruynseraede, Solid State Commun. **91**, 331 (1994); M. Baert, V. Metlushko, R. Jonckheere, V. V. Moshchalkov, and Y. Bruynseraede, Phys. Rev. Lett. **74**, 3269 (1995).

[10] W. Van Roy, Ph.D. thesis, K. University of Leuven, Belgium, 1995.

[11] H. J. Fink and A. G. Presson, Phys. Rev. **151**, 219 (1966); H. J. Fink and L. J. Barnes, Phys. Rev. Lett. **15**, 792 (1965).

[12] F. de la Cruz, H. J. Fink, and J. Luzuriapa, Phys. Rev. B. **20**, 1947 (1979).

[13] W. Klose, Phys. Lett. **8**, 12 (1964); R. A. Kamper, *ibid*. **5**, 9 (1963).

[14] A. A. Abrikosov, Sov. Phys. JETP **8**, 710 (1966).

[15] W. H. Press, B. P. Flannery, S. A. Teukolsky, and W. T. Vetterling, *Numerical Recipes in C* (Cambridge University Press, Cambridge, England, 1992), Chap. 17.3.

[16] G. N. Lance, *Numerical Methods for High Speed Computers*, (Iliffe & Sons Ltd., London, 1960), Chap. 3.10.

[17] D. Saint-James, E. J. Thomas, and G. Sarma, *Type II Superconductivity* (Pergamon Press, Oxford, 1969).